Physics Letters B 741 (2015) 316–319

Contents lists available at ScienceDirect

Physics Letters B

www.elsevier.com/locate/physletb

A magnetic trap for high-field seeking neutron spin states

Th. Brenner [a], S. Chesnevskaya [b], P. Fierlinger [b,*], P. Geltenbort [a], E. Gutsmiedl [b], T. Lauer [c], K. Rezai [d], J. Rothe [b], T. Zechlau [c], R. Zou [d]

[a] Institut Laue-Langevin, 38042 Grenoble Cedex 9, France
[b] Physik Department, Technische Universität München, D-85748 Garching, Germany
[c] Forschungsneutronenquelle Heinz Maier-Leibnitz, Technische Universität München, D-85748 Garching, Germany
[d] University of California at Berkeley, CA 94720, USA

ARTICLE INFO

Article history:
Received 20 October 2014
Accepted 18 December 2014
Available online 24 December 2014
Editor: D.F. Geesaman

ABSTRACT

A first experimental demonstration of a new type of magnetic trap for ultra-cold neutrons is presented. High-field seeking spin-states are trapped in a potential formed by the magnetic field of a straight wire and a repulsive coating on the wire surface. Life-times of the trapped neutrons of 60 s could be observed. This configuration can in principle be used to form bound states of the wave function on the surface of the wire to probe new forces at short distances. Further applications include the use as a guide and selector for perfectly polarized neutrons.

1. Introduction

Ultra-cold neutrons (UCN) are neutrons with velocities below ~ 7 m/s or few 100 neV kinetic energy [1,2]. Such neutrons experience total reflection on many material surfaces under any angle of incidence. This is due to the so-called Fermi-potential V_F, an effective potential caused by an average interaction with many nuclei:

$$V_F = \frac{2\pi\hbar^2}{m_n} Nb, \tag{1}$$

with N the number density of atoms, b the bound coherent scattering length of the atomic nuclei in the material and m_n the mass of the neutron. Further, the effect of gravity, $1.02 \cdot 10^{-7}$ eV per meter height, is comparable to the kinetic energy, as well as splitting of energy levels in magnetic fields:

$$V_B = \pm|\mu_n|B, \tag{2}$$

with $|\mu_n| \sim 6 \cdot 10^{-8}$ eV/T the magnetic moment of the neutron. As the Larmor-precession frequency is in many cases fast compared to changes in the magnetic field as seen by the neutron, the alignment of the polarization adiabatically follows the magnetic field lines [3]. Thus, once the particle enters a static magnetic field, it experiences a force which either repells low-field-seeking spin-states (LFS) from regions of high magnetic field, or attracts high-field-seeking spin-states (HFS) repsecitvely. Usually a combination of the interaction of neutrons with magnetic fields, Fermi-potential and gravity enables the construction of traps, where UCN can be confined for up to their beta-decay life-time. For a theoretical discussion on magnetic manipulation of neutrons see e.g. [4]. Also, magnetic trapping of neutrons around a very thin wire has previously been discussed theoretically [5,6]. Guides and traps for high-field seeking spin-states have been demonstrated previously in matter-wave optical applications [7–10], where neutral atoms are guided. In neutron physics, magnetic traps for LFS have been realized previously [11,12] and are used for the precise measurement of the life-time of the free neutron. However, trapping of HFS has only been demonstrated recently [13]. In this work, a new type of magnetic trap for UCN is presented. It is formed by a wire, with a variable strong current for radial magnetic confinement. Axial confinement is achieved by mirrors, which are mounted on the wire at both ends of the trapping region. For the case of a static magnetic field quantum mechanical bound states are expected on the surface of the wire, similarly to e.g. [14,15]. The wire is thick and thus the bound states are comparable to states forming on a flat surface. Such a configuration would be sensitive to new (gravity-like) forces at short distances and thus be an alternative pathway to search for physics beyond the standard model of particle physics. However, due to the small energy of such states, much improved statistics is required, which can be achieved in continuous operation and transmission through a cylinder-shaped collimator mounted around the wire. The concept further has potential

* Corresponding author.
E-mail address: peter.fierlinger@tum.de (P. Fierlinger).

http://dx.doi.org/10.1016/j.physletb.2014.12.041

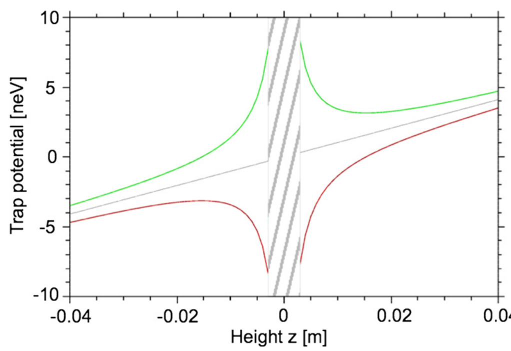

Fig. 1. Potential distribution as a function of vertical distance from the symmetry axis (position of the wire). The upper (green) curve corresponds to the potential that LFS experiences, the lower (red) curve applies to HFS. The hatched region between $z = \pm 0.003$ m is the volume occupied by the wire. Gravity tilts the vertical potential, as denoted by the solid (grey) line. (For interpretation of the references to color in this figure legend, the reader is referred to the web version of this article.)

applications as a guide for polarized extremely low energy neutrons or high brightness polarized beams with transverse velocities $v_T < v_c = \sqrt{2V_F/m_n}$, where V_F is the Fermi-potential of the wire surface.

2. Experimental apparatus

The trap was realized by a wire with a strong current I, which forms a radially increasing potential along the radius r for high-field seeking spin-states. In the case of a horizontal wire, the potential is in addition disturbed by gravity in z-direction:

$$V_{HFS}(r, z) = \frac{\mu_n \mu_0 I}{2\pi r} + m_n g z. \quad (3)$$

At the radius of the wire $r_0 = 0.003$ m, the potential makes a step according to the Fermi-potential V_F of the wire. The trapping potential for HFS and LFS is shown in Fig. 1. Here, one important parameter characterizing the trap is the distance from the wire at which gravity overwhelms the magnetic forces. In a horizontal setup, this happens at a critical radius

$$r_{crit} = \sqrt{\frac{|\mu_n| \mu_0 I}{2\pi m_n g}}. \quad (4)$$

With trap depth of 10^{-9} eV, similar to the kinetic energy of the trapped UCN, the neutron's trajectories are calculated using classical equations of motion. Filling the trap was realized by raising the current through the wire (and thus the magnetic trapping potential) while a continuous flux of neutrons ensured a constant density of UCN in the trapping region. High-field-seeking spin-states were trapped in a region between $r > r_0$ and $r < r_{crit}$ by ramping the magnetic field and thus lowering the magnetic potential during the passage of particles through this region. The trap was set up at the beam line PF2/UCN [16] Institute Laue-Langevin (ILL), Grenoble. A scheme of the experimental setup is shown in Fig. 2. Neutrons were supplied from the UCN turbine [17] into the neutron guide towards the experiment, separated by an aluminum foil with a $V_F = 54$ neV. This potential corresponds to a minimum velocity of all UCN entering the system $v_{crit} = \sqrt{2V_F/m} = 3.2$ m/s. The average neutron energy was then shifted to lower kinetic energies by placing the trap 1.6 m above the UCN exit port at the neutron turbine. The wire was horizontally inserted into the cylindrical neutron guide. It is comprised of a copper tube with 6 mm outer diameter and 4 mm inner diameter and a sputter-coating with a NiMo alloy composed of 85% Ni and 15% Mo. The coating has a high optical potential (238 neV) and is non-magnetic, its

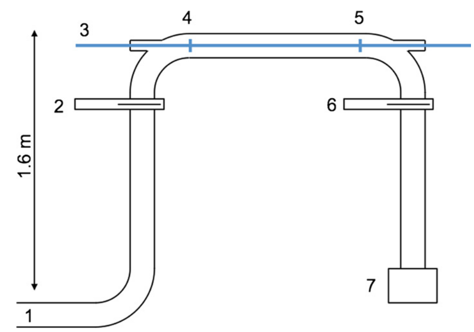

Fig. 2. Experimental apparatus for wire trapping. The trap was formed of neutron guides in vacuum with 0.07 m diameter. Neutrons entered the apparatus from the UCN turbine at ILL-PF2 [1] and were guided 1.6 m up through a shutter [2]. The wire that carried the current to form the trapping field [3] entered the guide through an insulated feedthrough and left the guide again after 1.3 m. At positions [4] and [5], reflecting copper mirrors with 0.03 m diameter were mounted on the wire with 0.54 m distance for axial confinement. This defines the axial length of the trap. Through the shutter [6] neutrons then left the volume to be counted in the detector [7].

non-depolarizing properties have been investigated previously [18, 19] and should not limit the storage of HFS for this experiment. Two coated copper discs with 0.03 m diameter were mounted on the wire for axial confinement. Additionally, cooling water with 3 bar pressure was supplied to the wire by an external source to combat electrical heating. Current was supplied by a DANFYSIK *System 8000* power supply with a maximum output of 2000 A at 2 V. The vacuum during the measurements was $< 3 \times 10^{-3}$ mbar. Neutrons were detected using a CASCADE detector [20], which is based on neutron conversion at a boron coated entrance window to charged particles for detection. The detector was located on the adjacent side of the guide 0.9 m below the trap so neutrons were accelerated by gravity to gain sufficient energy to enter the detector through an aluminum window. A layer of cadmium plates and an outer layer of borated polyethylene bricks was mounted to shield external background; together with two additional shutters along the neutron guide between the turbine and the setup the environmental noise after shielding decreased to ~ 13 mHz for most of the actual measurements. Operation of shutters, magnet power supply and the detector readout was fully automatic to enable cyclic measurement sequences.

3. Measurement

A numerical simulation of the trapping procedure has been performed. Initial momenta and positions of UCN inside the guide have been assumed to be random. The velocity distribution of the neutrons is assumed to be similar to Ref. [17]. The trajectories of the neutrons are calculated using a Runge–Kutta 8th-order algorithm in a time-varying magnetic potential. Various tests of the parameters used for the simulations have been performed. For a wide range of realistic parameters, e.g. for the diffuse scattering probability on the walls or the mechanical precision of the wire and the discs, the performance of the trapping procedure showed no strong dependence. A simulation of critical trapping parameters is shown in Fig. 3: the trapping probability for different neutrons in the guide with different velocities is plotted on the left with parameters similar to the actual measurement. A velocity of 1 m/s corresponds roughly to 6 neV kinetic energy (about equal to the trap depth). The average velocity of the trapped particles is ~ 0.3 m/s. On the right, the dependence of the trapping probability on the final current is shown with a constant ramp speed of 250 A/s. The trapping efficiency is proportional to the velocity distribution in the guide volume. The requirement for large cur-

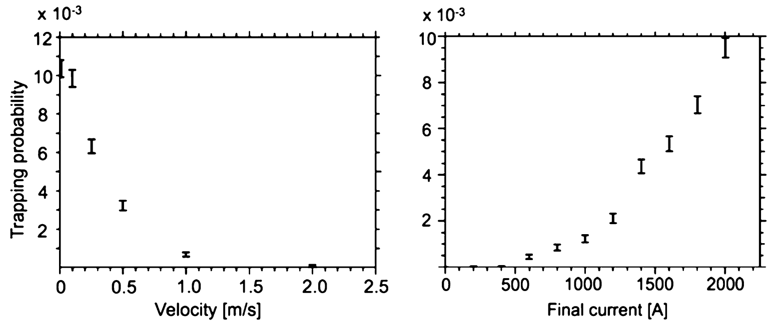

Fig. 3. Left: simulated trapping probability as a function of neutron velocity; here, the current was ramped from 0 A to 1400 A with a ramp of 250 A/s. Right: trapping probability for 0.5 m/s UCN with varying final current; here, the current was ramped from 0 A to the final current with a ramp of 250 A/s.

rents also follows from this behavior. Further simulations show the almost linear dependence of the trapping efficiency on the current-ramp rate, which is on the order of 5×10^{-3} for 100 A/s, 1×10^{-2} for ~ 220 A/s and 1.5×10^{-2} for 450 A/s for 1400 A fixed maximum current.

A typical trapping sequence started with filling the neutron guides to equilibrium density for 40 s. Note that the time constant to reach equilibrium density is only few seconds for the average UCN spectrum from the turbine, but on the order of 20–30 s for the neutrons with velocities of 0.3 m/s. Then the current was ramped up to trap HFS. Internal heating of the power supply limited the current through the wire to 1400 A. For the actual measurement a ramp of 240 A/s was chosen to optimize trapping efficiency as well as prevent internal overheating of the power supply. After ramping, the shutter (item [2] in Fig. 2) and additional shutters along the beam line were closed. Then, all neutrons in the volume of the guide that were not trapped were counted in the detector. After a storage period for trapped neutrons of 60 s (when the non-trapped neutrons have left the volume) the current was switched off and the trapped neutrons were counted in the detector. Measurements were performed in an alternating sequence of runs with current and otherwise identical runs but with zero current. Due to the small count rate, this was critical to monitor background during data-taking periods.

The expected number of trapped neutrons was estimated from the number of neutrons found in the guide volume, about 36 000 after filling: assuming energies up to 210 neV (the Fermi potential of stainless steel) with a linearly increasing distribution and a shift of the spectrum by 160 neV due to gravity, only 270 of these have velocities below 1 m/s. Using the calculated trapping probability for UCN with 0.4 m/s, 1.5 trapped UCN per run are expected. Losses due to wall collisions are $\sim 10^{-6}$ per wall collision for kinetic energies of < 1 neV, the depolarization rate for the NiMo coating of the wire is below 10^{-5} per wall collision without known energy dependence. Emptying of the trap had a time constant of ~ 25 s. For this estimate (consistent with data), we used an average velocity of 0.3 m/s, a velocity in guide direction of about 0.2 m/s and a characteristic distance from the trap to the detector of 2 m. With the signal distributed over 40 s during emptying, this corresponds to an expected count rate of 25 mHz. However, this is dependent on the unknown exact form of the UCN velocity distribution.

Fig. 4 shows a sum of 119 sets of subsequent measurements with and without current. The rate is normalized to counts per second per run, averaged over 10 s. The time $t = 0$ on the x-axis corresponds to the time when the current was switched off and the trap was emptied. The background measurements are identical cycles (including the same time constants), but with current set to zero and thus without filling of the trap. The filled circles (red color) show the count rate of UCN that left the guide 60 s after the

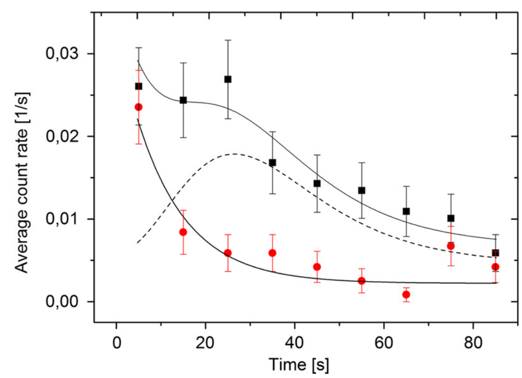

Fig. 4. Neutron count rate in the detector after the magnetic field in the trap is switched off (at $t = 0$). Data runs (with current) are denoted by the square (black), background runs (without current but otherwise identical conditions) are denoted by the circles (red). The background obeys a purely exponential fit. The signal is fitted by a superposition of the underlying exponential decay of the background and a peak. To guide the eye, the dashed line illustrates the fit function for the peak alone. It is composed of a rise time component and an exponential decay. For an explanation of the fit see text. (For interpretation of the references to color in this figure legend, the reader is referred to the web version of this article.)

shutters were closed: the rate of UCN which reach the detector is exponentially decreasing and finally approaches a flat constant background level. The solid line is the corresponding exponential fit with an offset. The filled squares (black color) show the count rate after the current was switched off and the trapped UCN were counted in the detector. Also in this case an exponentially decreasing rate can be observed, with a peak of trapped UCN The result is fitted by superimposing a peak on the identical exponential background fit. The peak is composed of an exponential rise and an exponential decay, resulting in an overall duration of the emptying procedure. This characteristic shape has been simulated, with the time constants for rise and decay being correlated and dependent on the diffuse scattering behavior of the overall guide system. As diffusion is an unknown quantity here, the time constant is simply matched to best fit the result with a reduced $\chi^2 = 0.5$. Its statistical significance is $> 8\sigma$ above background and corresponds to the estimated signal from simulation. The data is selected from a series of subsequent trapping and background measurements, while the background drifted from 10–50 mHz during the measurement period. A cut was applied to remove sets of six subsequent data- and background-runs around every measurement where the background measurements exceeded 20 mHz. The stability of this procedure was confirmed by changing the size of a window around which sets of data were dismissed. The background depended on the shutters along the beam line, which did not perfectly close and thus caused a constant background. The temporally variable contribution to the background seemed to depend on the state of the guides inside the UCN turbine. The result also indicates that the depolarization probability per wall collision for < 5 neV HFS on non-depolarizing NiMo layers is $< 10^{-5}$ per wall collision, which has not been tested previously. Such a possible energy-dependent behavior has been subject to previous investigations [21,22], although for significantly higher energies and larger magnetic fields.

4. Conclusions

A new type of magnetic trap for high-field-seeking spin-states has been realized and its operation principle has been demonstrated for the first time. The concept of using a rotation-symmetric potential around a wire also has potential future applications as a specialized polarized neutron guide or to probe new forces of nature at short distances. We wish to acknowledge the great support at the Meier-Leibnitz Laboratory in Garching and at the Institute Laue-Langevin in Grenoble. This work was supported by the DFG Cluster of Excellence ‘Origin and Structure of the Universe’. K. Rezai was supported by the generous stipend of the Qualcomm foundation.

References

[1] E. Fermi, Ric. Sci. 7 (2) (1936) 13.
[2] Ya.B. Zeldovich, Sov. Phys. JETP 6 (1959) 1389.
[3] R. Golub, D.J. Richardson, S.K. Lamoreaux, Ultra-Cold Neutrons, Adam Hilger, Bristol, 1991.
[4] V.V. Vladimirskii, Sov. Phys. JETP 12 (1961) 740.
[5] R. Blümel, K. Dietrich, Phys. Lett. A 139 (1989) 236.
[6] R. Blümel, K. Dietrich, Phys. Rev. A 43 (1991) 22.
[7] J. Schmiedmayer, in: G. Magerl (Ed.), XVIII Int. Conf. on Quantum Electronics: Technical Digest, vol. 9, Technische Universität Vienna, Vienna, 1992, p. 284.
[8] J. Schmiedmayer, Phys. Rev. A 52 (1995) R13.
[9] J. Schmiedmayer, Appl. Phys. B 60 (1995) 169.
[10] W. Wing, Prog. Quantum Electron. 8 (1984) 181.
[11] V.F. Ezhov, A.Z. Andreev, G. Ban, B.A. Bazarov, et al., Nucl. Instrum. Methods A 611 (2009) 167.
[12] W. Paul, F. Anton, L. Paul, S. Paul, et al., Z. Phys. C 45 (1989) 25.
[13] M. Daum, P. Fierlinger, B. Franke, P. Geltenbort, et al., Phys. Lett. B 704 (2011) 456.
[14] V.V. Nesviszhevsky, H.G. Börner, A.K. Petukhov, H. Abele, et al., Nature 415 (2002) 297.
[15] T. Jenke, P. Geltenbort, H. Lemmel, H. Abele, Nat. Phys. 7 (2011) 468.
[16] www.ill.eu/pf2/.
[17] A. Steyerl, H. Nagel, F.-X. Schreiber, K.-A. Steinhauser, et al., Phys. Lett. A 116 (1986) 347.
[18] S. Gosh, N. Das, A. Mookerjee, J. Phys. Condens. Matter 10 (1998) 11773.
[19] V.K. Ignatovich, The Physics of Ultracold Neutrons, Oxf. Ser. Neutron Scatt. Condens. Matter, vol. 5, Clarendon Press, Oxford, 1990.
[20] www.n-cascade.com.
[21] J. Karch, Diploma thesis, Univ. Mainz, 2011.
[22] G. Kessler, Diploma thesis, TU München, 2011.